Anti-lock braking control design using a nonlinear model predictive approach and wheel information

Pretagostini, Francesco; Shyrokau, Barys; Berardo, Giovanni

DOI
10.1109/ICMECH.2019.8722841

Publication date
2019

Document Version
Final published version

Published in
Proceedings - 2019 IEEE International Conference on Mechatronics (ICM 2019)

Anti-lock braking control design using a Nonlinear Model Predictive approach and wheel information

Francesco Pretagostini
Department of Cognitive Robotics
TU Delft
Delft, The Netherlands
f.pretagostini@student.tudelft.nl

Barys Shyrokau
Department of Cognitive Robotics
TU Delft
Delft, The Netherlands
b.shyrokau@tudelft.nl

Giovanni Berardo
Chassis control department
Toyota Motor Europe
Brussels, Belgium
giovanni.berardo@toyota-europe.com

***Abstract* — Since several decades anti-lock braking systems rely on rule-based control strategies. Extensive literature review highlighted the possibility that significant improvements could be achieved if ABS controllers were redesigned taking advantage of the technological improvements achieved in the last decade. This work aims to verify this statement and quantifying the potential improvement by design of a novel ABS algorithm. The controller, based on state-of-the-art hardware, uses a Model Predictive Control (MPC) approach and potentially available wheel information as the pillars of its design. The newly proposed ABS is then tested on Toyota's high-end vehicle simulator and benchmarked against its industrial counterpart. A comprehensive set of manoeuvres, including friction jumps and rough road braking scenarios, is deployed to assess performance and robustness of the presented design. The analysis showed substantial reduction of the braking distance and improved steering-ability. Furthermore, robustness against external factors is demonstrated to be comparable with the industrial benchmark.**

Keywords—Antilock Braking System, wheel slip control, Model Predictive Control, load sensing, high-end simulation

I. INTRODUCTION

Anti-Lock Braking System (ABS) is an active safety technology used to control wheel dynamics during severe braking. The system aims at maximizing braking performance while keeping the vehicle's ability to steer. The ABS control objective is practically achieved by monitoring the applied brake torque by means of pressure modulation.

Being a safety system, ABS must be robust to all possible conditions that could be encountered, such as different friction surfaces, uneven roads and sudden changes in adhesion. Additionally, the dynamics of the wheel slip becomes faster as the velocity decreases, and it is therefore key to counteract this effect [1]. Moreover, the vehicle velocity and thus longitudinal wheel slip signal, as well as the tire-road friction coefficient require estimation. Lastly, the plant to be controlled (elastically suspended wheel, braking servo system and disc-pad interaction) presents significant nonlinearities and delays which limit the controller's bandwidth. Besides, the main nonlinearity arises from the strong tire saturation behaviour.

Since the first reliable automotive application by Bosch in 1978 [1, 2] a wide variety of approaches have been proposed for ABS control. In literature, two control variables have traditionally been used: wheel acceleration $\dot{\omega}$ and longitudinal wheel slip λ.

The angular acceleration approach has the main advantage that this can be measured with a wheel encoder. Furthermore, controllers of this type are able to keep the wheel slip in a neighbourhood of the optimal point without explicitly using the value of optimal wheel slip.

On the other hand, wheel slip control is simpler from a dynamical point of view and less sensitive to friction coefficient estimation errors. Moreover, slip control has the feature that the applied torque converges to a fixed value, hence, it shows no oscillations compared to wheel acceleration control [4], [5]. Nonetheless, the slip measurement requires the estimation of vehicle speed. Therefore, noise sensitivity of the controller is a critical issue [1]. Additionally, set selection point is extremely crucial, and, since it is impossible to find a unique value for every road condition, a set point adaption must be implemented [3].

ABS could be made more robust and less complex if the tire longitudinal forces were used. Wheel force information, in fact, would allow to easily estimate the friction coefficient peak [6]. Additionally, when used in the formulation of model-based, optimization-based control approaches, tire forces' availability allows to eliminate the need of a tyre model and, with it, some nonlinearities and tedious trigonometric functions that may slow down the optimization solver. Load-sensing bearings allow to reconstruct wheel forces with sufficient accuracy and bandwidth and thereby enable their application in vehicle dynamics control in the near future [7]. Based on the above-mentioned considerations, a slip-based approach augmented with the use of wheel force information is investigated in this work.

The control strategy was selected after in-depth analysis of the main ABS control trends proposed by researchers and OEMs. A brief summary of the conclusions is now presented; nonetheless, more detailed discussions can be found in [8, 9]. Two macro directions were identified in literature: the first one, comprising of dynamic threshold-based, fuzzy logic and neural network controllers, achieves the control objective by discretely modulating brake pressure for each wheel; the second one, including PID, robust, sliding mode, optimal and model predictive controllers, assumes the possibility of continuously modulating brake pressure.

Among continuous controllers, MPC represents an opportunity to improve dynamic performance and robustness of the current state-of-the-art controllers; however, the prediction and optimization behind it make it computationally very intensive. It is believed that the use of wheel force measurements in the prediction, in place of a tire model, will significantly improve the MPC real time capability. The goal of this work is thus to design a novel ABS model predictive controller augmented with wheel information and quantify the potential improvement over nowadays rule-based systems.

978-1-5386-6959-4/19/$31.00 ©2019 IEEE

In the next sections, an overview of the steps performed to achieve the research objective is given. First, the proposed controller is explained in section II; a brief introduction of the simulation set-up is then given in section III; assessment of the newly proposed controller is subsequently described in section IV; section V discusses some of the results obtained; lastly, important conclusions about the feasibility and performance of the proposed control strategy are drawn in section VI.

II. PROPOSED ABS CONTROLLER

Model Predictive Control uses a dynamic model of the system to predict its evolution over a finite time interval, called the prediction horizon (T_P). The predicted behaviour is then optimized via control inputs with respect to a given optimality criterion (J) reflecting the control objectives. The criterion is formulated as a cost function and system constraints and solved at each sampling period. After computation of the optimal control sequence, only the first control move is applied in closed loop. In the next sampling interval, the entire process is repeated using the most recent state measured, a process known as receding horizon control. Because of the high nonlinearity of the slip dynamics, to guarantee sufficient accuracy of predictions, and therefore avoid large plant-model mismatch, a nonlinear model is used for predictions.

The model, shown in (1), consists of nine differential equations: four equations describe the wheel slip dynamics of each wheels ($\dot{\lambda}_{ij}$); an additional four augmentation equations ($\dot{T}_{b_{ij}}$) allow controlling the torque rate ($dT_{B_{ij}}$) instead of the brake torque; lastly one equation describes the chassis longitudinal dynamics $\dot{v}$. Effects related to brake actuator dynamics and longitudinal weight transfer are also considered. Electro-hydraulic brake system behaviour can be represented by a first order dynamics with time constant τ. On the other hand, longitudinal weight transfer can be approximated by its static part. Lastly, online feed of wheel force data allows complete description of the tire dynamics.

$$\begin{bmatrix} \dot{T}_{b_{FL}} - dT_{b_{FL}} \\ \dot{\lambda}_{FL} + \frac{1-\lambda_{FL}}{v\left(\frac{m_{fr}}{2} + \frac{m_s a_x h}{2L}\right)} + \frac{R_w^2}{I_w v} + F_{x_{FL}} - \frac{R_w}{v I_w}\left(dT_{b_{FL}}\tau + T_{b_{FL}}\right) \\ \dot{T}_{b_{FR}} - dT_{b_{FR}} \\ \dot{\lambda}_{FR} + \frac{1-\lambda_{FR}}{v\left(\frac{m_{fr}}{2} + \frac{m_s a_x h}{2L}\right)} + \frac{R_w^2}{I_w v} + F_{x_{FR}} - \frac{R_w}{v I_w}\left(dT_{b_{FR}}\tau + T_{b_{FR}}\right) \\ \dot{T}_{b_{RL}} - dT_{b_{RL}} \\ \dot{\lambda}_{RL} + \frac{1-\lambda_{FL}}{v\left(\frac{m_{rr}}{2} - \frac{m_s a_x h}{2L}\right)} + \frac{R_w^2}{I_w v} + F_{x_{RL}} - \frac{R_w}{v I_w}\left(dT_{b_{RL}}\tau + T_{b_{RL}}\right) \\ \dot{T}_{b_{RR}} - dT_{b_{RR}} \\ \dot{\lambda}_{RR} + \frac{1-\lambda_{RR}}{v\left(\frac{m_{rr}}{2} - \frac{m_s a_x h}{2L}\right)} + \frac{R_w^2}{I_w v} + F_{x_{RR}} - \frac{R_w}{v I_w}\left(dT_{b_{RR}}\tau + T_{b_{RR}}\right) \\ \dot{v} - \frac{F_{x_{FL}} + F_{x_{FR}} + F_{x_{RL}} + F_{x_{RR}}}{m_t} \end{bmatrix} = \begin{bmatrix} 0 \\ 0 \\ 0 \\ 0 \\ 0 \\ 0 \\ 0 \\ 0 \end{bmatrix} \quad (1)$$

In (1) $F_{x_{ij}}$ is the longitudinal tire force, a_x the longitudinal acceleration, v the chassis velocity, I_w the wheel's rotational inertia, L the wheel base, R_w the tire's loaded radius, m_s the sprung mass, m_{fr} and m_{rr} the portions of the total mass resting on the front and rear axles respectively.

The state vector is then:

$$x = \left[T_{b_{FL}}, \lambda_{FL}, T_{b_{FR}}, \lambda_{FR}, T_{b_{RL}}, \lambda_{RL}, T_{b_{RR}}, \lambda_{RR}, v\right]^T \quad (2)$$

Optimization-based brake torques, $dT_{b_{ij}}$, result from iteratively solving a constrained Optimal Control Problem (OCP). In its general form and assuming the state to be measurable, the OCP is formulated as follows:

$$\begin{aligned} &\text{minimize}_{y(\cdot),u(\cdot)} \underbrace{\int_{t_0}^{t_0+T_p} \left(\|y(t) - y_{ref}(t)\|_Q^2 + \|u(t) - u_{ref}(t)\|_R^2\right)dt + \|y(t_0 + T_P) - y_{ref}(t_0 + T_P)\|_P^2}_{J} \\ &x(t_0) = \bar{x}_0 && \text{Initial conditions} \\ &\dot{x}(t) = f\big(x(t), u(t)\big) && \text{Vehicle dynamics} \\ &y(t) = g\big(x(t), u(t)\big) && \text{Output mapping} \\ &x_{min}(t) \le x(t) \le x_{max} && \text{State constraint} \\ &u_{min}(t) \le u(t) \le u_{max} && \text{Actuator contraint} \\ &Q \in R^p_{\ge 0}, \quad R \in R^m_{\ge 0}, \quad P \in R^p_{\ge 0} \end{aligned} \quad (3)$$

The solution of the OCP is the result of minimizing the cost function J, in which: Q and P are non-negative definite weight matrices penalizing the deviations of the outputs (y) from their reference values y_{ref}, and R is positive definite weight matrix penalizing the deviations of the inputs u from their reference values u_{ref}. Weight matrices can therefore be used as tuning parameters.

State and input constraints, reported in Table I, were chosen according to the following reasoning:

- Since the focus is braking dynamics, the slip is constrained such that solutions are searched in the range between 0 and 1.
- The lower bound for the chassis velocity is set to 0 to prevent the vehicle from going backwards, while the upper-bound is selected equal to the vehicle's maximum speed.
- The brake torques' lower bound is placed at 0 Nm as negative number would mean that a driving torque is applied. The upper-bound is again set at the system's maximum capability; Given the different sizing of front and rear brakes, two values are found.
- Limits for the brake torque rates are also set at the pressure actuator's limits. Since the EHB pressure increase rate is around 1300bar/s and assuming the system is 30% slower in damping pressure, the torque rate bounds are set to $\dot{T}_{b_{MAX}}$= 42000Nm/s and $\dot{T}_{b_{MIN}}$ = 30000Nm/s. As for stability reasons it is advisable for rear wheels to follow the front ones in the event of a lock up, the rear pressure increase rate is reduced for the rear axle.

TABLE I. STATE AND INPUT BOUNDS

Variable	*Unit*	*Lower-bound*	*Upper-bound*
$T_{b_{fr}}$	[Nm]	0	3500
$T_{b_{rr}}$	[Nm]	0	1700
λ_{ij}	[-]	0	1
v	[m/s]	0	53
$\dot{T}_{b_{fr}}$	[Nm/s]	-35000	42000
$\dot{T}_{b_{rr}}$	[Nm/s]	-35000	35000

The tool used as modelling environment to define the optimal control problem is ACADO Toolkit. ACADO is an open-source software environment for dynamic optimization which supports self-contained C code [10]. Its most appealing features is the task scheduling of the Real Time Iteration (RTI) scheme which splits one iteration into two phases: a preparation phase, where the NLP is linearized, discretized and condensed; and a feedback phase, where the condensed QP is solved. Since operations are independent from the optimization's initial state (x_0), the

preparation can be executed before measurements arrive. In this way, real-time performances within the milli- or micro-seconds range can be achieved depending on the application [11].

The OCP problem is solved by the dense QP solver qpOASES, an open source structure-exploiting active-set solver that supports warm start particularly suited for MPC applications [12]. The most important solver settings are reported in Table II, the complete list can be found in [13].

TABLE II. IMPORTANT CONTROLLER SETTINGS

Variable	*Value*
Prediction horizon (T_p)	100 ms
Sampling time (T_S)	5 ms
Controller frequency (f_{CTRL})	250 Hz

As mentioned, the MPC is the core of this novel ABS formulation; nonetheless, other elements are also important for its correct behaviour. The full controller structure is shown in Fig. 1.

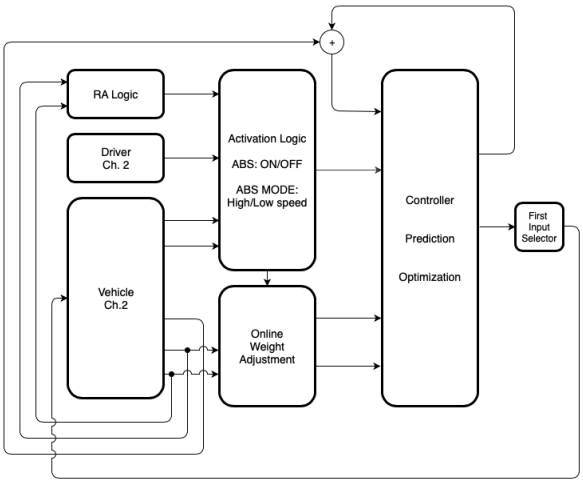

Fig. 1. ABS controller scheme.

The reference adaption block reads longitudinal $F_{x_{ij}}$ and normal force $F_{z_{ij}}$ at each step and, after calculating the friction coefficient μ_{ij}, outputs the target wheel slips λ_{ij} based on a 3D-map obtained from tire testing. The slip targets, together with other signals coming from the vehicle and driver subsystems, are then passed to the activation logic.

The activation logic is responsible for cycling through three possible controller states: ABS Off, ABS On, ABS On - Low Speed. Based on a state machine, the controller's mode and target state are selected. Whenever the ABS is inactive the NMPC acts as a driver brake request follower. Activation of the ABS controller is triggered based on some predefined wheel deceleration thresholds for front and rear wheel pairs. In a range from 1 m/s to V_{MAX}, the ABS operates as a slip target follower. On the other hand, below 1 m/s, where the wheel dynamics is too unstable to control, the brake torque is kept constant to avoid any under-braking.

The selected control mode is implemented by the online weight adjustment logic via selection of the entries of the weight matrices Q, P and R (where R is equal to Q). In this formulation Q and P are diagonal matrices containing state weights and control weights respectively. When the driver is in control, the MPC is forced to track the driver demand using the following weight entries:

$$\left[W_{T_{b_{fr}}}, W_{\lambda_{fr}}, W_{T_{b_{rr}}}, W_{\lambda_{rr}}, W_v, W_{\dot{T}_{b_{fr}}}, W_{\dot{T}_{b_{rr}}}\right] \tag{4}$$
$$= [50\,, 0\,, 50\,, 0\,, 0.5 \times 10^{-5}, 1 \times 10^{-5}]$$

On the other hand, in low speed ABS mode, the controller is made inert by using:

$$\left[W_{T_{b_{fr}}}, W_{\lambda_{fr}}, W_{T_{b_{rr}}}, W_{\lambda_{rr}}, W_v, W_{\dot{T}_{b_{fr}}}, W_{\dot{T}_{b_{rr}}}\right] \tag{5}$$
$$= [0\,, 0\,, 0\,, 0\,, 0\,, 5 \times 10^5\,, 5 \times 10^5]$$

Lastly, when the ABS is working in its normal mode, the controller acts as a slip reference tracker. Since the vehicle velocity acts as a time-scale factor for the slip dynamics [1], cost weights are defined so to track the slip target with an increasingly larger control effort to cope with the progressively higher slip frequency:

$$\left[W_{T_{b_{fr}}}, W_{\lambda_{fr}}, W_{T_{b_{rr}}}, W_{\lambda_{rr}}, W_v, W_{\dot{T}_{b_{fr}}}, W_{\dot{T}_{b_{rr}}}\right] \tag{6}$$
$$= [0\,, 5 \times 10^8\,, 0\,, 3.7 \times 10^7\,, 0\,, f_{fr}(v)\,, f_{rr}(v)]$$

Where: $f_{fr}(v)$ and $f_{rr}(v)$ are two monotonically decreasing functions.

Current state, target state, online force measurements and cost weights are then sent to the NMPC which calculates the optimal inputs. The prescribed brake torques then act as a target for the low-level ABS controller which operates the hydraulic unit. Corner pressures are then applied to the vehicle which closes the loop.

III. VEHICLE SIMULATOR

Performance of the proposed controller was assessed on the high-end simulation set-up, shown in Fig. 2. Each of the main vehicle subsystems was developed in the appropriate simulation suite, namely, MATLAB Simulink for the controller, Simpack for the vehicle, Dymola for the brake system and MF Swift for the tire. The models were then interconnected to replicate full vehicle behaviour.

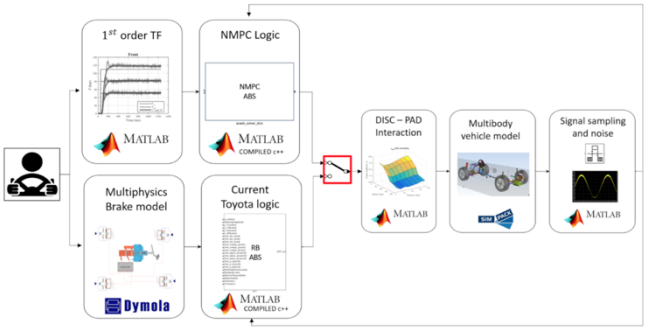

Fig. 2. Vehicle co-simulation layout

The vehicle model is realized following a multibody approach and largely validated against test data. Flexible bodies behaviour subsystems compliance were measured on dedicated test benches and reproduced either by correct modelling of the element (e.g. for springs and dampers) or by the insertion of compliant constraints at specific locations. Hydraulics brake system behaviour is replicated following a multiphysics approach, while for the EHB, where the nonlinearity is less, a first order TF was sufficient. The Short Wavelength Intermediate Frequency Tire (SWIFT) model, described in [14], was used in combination with a detailed tire property file. Lastly, the approach taken to reproduce sensor behaviour is to alter the information coming from the simulation so to match signal quality identified by the sensor's data sheet.

Validation was first performed for each subsystem and later in co-simulation. Longitudinal vehicle behaviour with the rule-based controller in-the-loop was correlated against EBD and ABS braking on track. Simulation output from 130-0 km/h high friction

braking is compared to six equivalent tests in Fig. 3. As can be seen, overall behaviour and pressure cycles, are closely matched. Deviations at low speed are caused by the tire not being tested in the lower speed range while generating the tire property file.

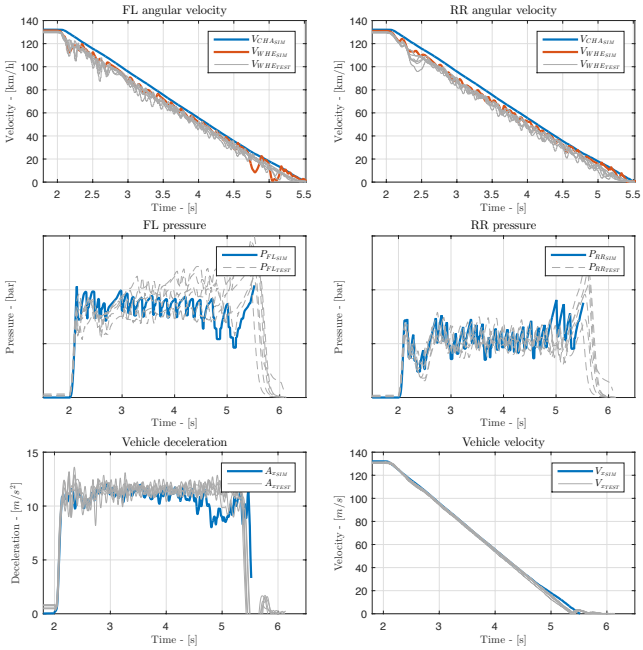

Fig. 3. ABS braking validation results

IV. ASSESSMENT

To assess the proposed controller and identify the performance margins compared to industrial solutions, the NMPC is benchmarked against a rule-based logic provided by Toyota. The two controllers are then simulated on eight scenarios, presented in Table III. In addition to smooth road braking, performance during friction transitions and on rough roads was also evaluated. Friction jumps follow the homologation rules mandated by the European UN transport division. Rough pavements were obtained using laser-scanning techniques on existing road sections.

Since the control blackbox used as a benchmark contained a series of other assistance systems together with ABS (e.g. VSC), simulation scenarios were selected so to only trigger the ABS. That is: reference trajectory was a straight line. Nonetheless, in case some yaw is caused by the controller actions, the driver model is tuned to countersteer as non-professional driver would do.

TABLE III. ABS BRAKING SCENARIOS

	Initial Velocity [km/h]	*Exit Velocity [km/h]*	*Avg. friction [-]*	*Surface layout*
Dry asphalt	130	0	0.9	Smooth
Wet asphalt	90	0	0.7	Smooth
Packed snow	40	0	0.3	Smooth
μ-jump	120	0	1.1 0.6	Smooth
μ-jump	60	0	0.75 → 0.35	Smooth
μ-jump	70	0	0.3 → 1	Smooth
Red bricks	70	0	0.65	Rough
Belgian stones	40	0	0.3	Rough

Understanding the relative margins with respect to the rule-based benchmark and where these originate was achieved by implementing effect-related performance indicators. Different KPI sets apply to each of the three groups of manoeuvres. Each indicator and the aspect it focuses on is listed in this paper, nonetheless, a more detailed explanation can be found in [13].

Steady state and transient performances, as well as human factors and actuator wear, are evaluated on smooth roads by the following KPPI set:

- ABS index of performance – Overall braking

$$\text{ABSIP} = \frac{d_{ABS}}{d_{Skid}}$$

- Brake distance – Overall Braking

$$\text{BD} = \int_{t_i}^{t_f} v_{CHA}\,dt$$

- Mean fully developed deceleration – Steady state

$$\text{MFDD} = [\bar{a}_x]_{0.05V_0}^{0.9V_0}$$

- ABS efficiency – Steady state

$$\eta_{ABS} = \frac{[\bar{a}_x]_{0.05V_0}^{0.8V_0}}{\bar{\mu}g}$$

- Peak-to-peak – First control cycle

$$\omega_{peak} = \sum_k \frac{\omega_{max,k} - \omega_{opt,k}}{\omega_{max,k}}\,;\, k = [FL, FR] \wedge [RL, RR]$$

- Integral time-weighted average of longitudinal jerk – Comfort

$$\text{ITAE}_{J_x} = \int_{t_i}^{t_f} t|J_x|\,dt$$

- Integral torque variation – Actuator wear

$$\text{IACA}_{T_b} = \int_{t_i}^{t_f} \sum_k |\dot{T}_{b,k}|\,dt\,;\, k = [FL, FR, RL, RR]$$

- Integral pitch variation – Driver distance perception

$$\text{IPV} = \int_{t_i}^{t_f} |\dot{\psi}|\,dt$$

Performance metrics used for the friction jumps are only focused on investigating the controllers' behaviour in relation to the friction transition. Two key aspects here are transient performance and lateral stability and they are:

- Mean deceleration at jump – Underbraking after jump

$$\bar{A}_{x,jump} = \int_{i_{jump}}^{f_{jump}+1s} a_x\,dt$$

- Minimum deceleration at jump – Underbraking at jump

$$A_{x,min} = \min[a_x]_{i_{jump}}^{f_{jump}}$$

- Recovery time – Underbraking after jump

$$T_{rec} = [t]_{i_{jump}}^{\pm 5\%\bar{A}_x}$$

- Peak-to-peak – Fist control cycle after jump

$$\omega_{peak_{jump}} = \sum_k \frac{\omega_{max,k} - \omega_{opt,k}}{\omega_{max,k}}\,;\, k = [FL, FR] \wedge [RL, RR]$$

- Maximum yaw rate at jump – Lateral stability

$$\dot{\psi}_{MAX} = \max[\dot{\psi}]_{i_{jump}}^{f_{jump}}$$

For rough roads some of the indicators for smooth ones are reused, however the metric is now is their change with respect to an equivalent manoeuvre performed on a smooth surface.

V. RESULTS

Detailed results for each of the eight ABS braking scenarios can be found in [13]; however, one per group will be shown here. Specifically: smooth dry asphalt, friction jump from dry-wet, and Belgian stones. For the friction transition the full analysis procedure is discussed, while for the other two scenarios, only a spider plot summarizing the findings is examined.

A first general understanding of the manoeuvre outcome is achieved by looking at the time-histories of the main signals of interest. Referring to Fig. 4, it is clear how after the controller activates, front brake torques are kept increasing to take advantage of the longitudinal weight transfer while rear ones are reduced. When the vehicle starts to pitch back the behaviour is reversed. Steady state would eventually be reached; however, at 2.5s the friction jump is experienced and brake torques readily reduced. Thanks to predicted behaviour optimization, underbraking is limited and the torques converge to their optimal value net of vehicle pitching.

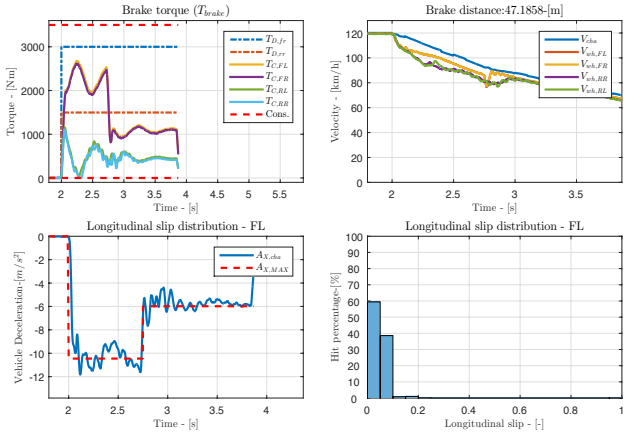

Fig. 4. Friction jump dry-wet time histories – NMPC.

Looking at the acceleration plot it is evident how the controller manages to stay very close to the physical maximum, both before and after the transition. Comparison between the wheel speeds and vehicle speed, shown in the top-right graph of Fig. 5, highlights the absence of the typical rule-based ABS control cycles. The longitudinal slip distribution graph of the front-left wheel points out how the slip is contained in a narrow band close to its optimal value; here in fact, two defined peaks, each associated with a specific friction coefficient, are identified. Moreover, very limited density is seen outside the stable area of the slip-force curve.

TABLE IV. FRICTION JUMP DRY-WET - ABSOLUTE KPI READINGS

	Rule-based	***NMPC***
$A_{x,min}$@jump $-$ [m/s^2]	2.52	4.38
$T_{recovery}$ $-$ [ms]	580	360
$\bar{A}_x$ $-$ [m/s]	4.07	5.88
Peak to Peak front $-$ [%]	66.60	14.67
Peak to Peak rear $-$ [%]	26.77	13.35
$\dot{\psi}_{MAX}$ $-$ [deg/s]	1.83	0.93

Using the previously presented metrics, the result can now be further analysed, and aspect-specific readings, shown in Table IV, produced. The minimum longitudinal acceleration at the jump reveals considerably less underbraking in response to the friction change for the NMPC controller with respect to its rule based equivalent. Similarly, the time needed to regain steady state is also noticeably less. As a result, the mean deceleration value sizably higher. Peak-to-peak metrics show how the first control cycle after the jump is deeper for the benchmark. Lastly, although lateral stability is retained in both cases, the maximum yaw rate underlines the superiority of the proposed approach also on this aspect.

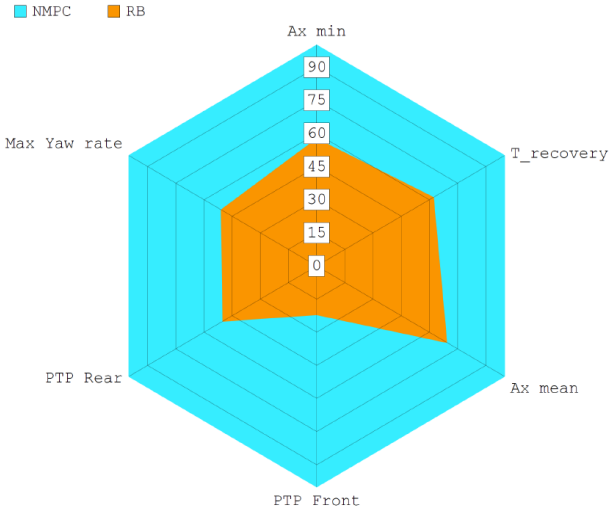

Fig. 5. Friction jump dry-wet – Relative KPI readings

In order to have a good understanding of how the relative gain originates, each KPI is then normalized to 100% for the best performing controllers, and relative performance is plotted on a spider chart. Figure 5 shows how, for this specific manoeuvre, the performance advantage is well distributed across all aspects. This is not the case for Fig. 6, showing the relative results for the dry asphalt braking from 130km/h. Here, although the NMPC is outperforming the current logic generally all the simulated manoeuvres, its main advantage is in the absence of first cycle overshoot, as particularly evident from the peak-to-peak indicators. Surely however, as a much larger portion of the braking manoeuvre is spent in stationary conditions fewer percentage points of difference in steady state performance also correspond to a remarkable improvement. Jerk and pitch related indices also reveal a substantial human factors gains. Moreover, the IACA, clears the concerns about actuator wear.

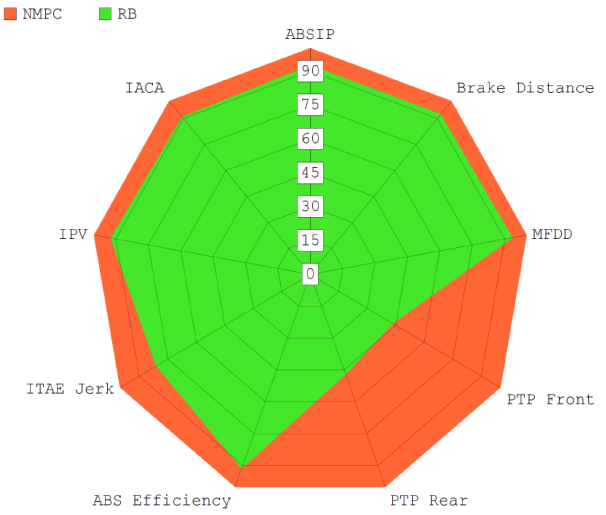

Fig. 6. Smooth dry asphalt braking – Relative KPI readings

On Belgian cobblestones, shown in Fig. 7, the NMPC is again outscoring the benchmark on overall braking performance deterioration; despite this, considerably higher torque fluctuations are needed to achieve it, as seen from the IACA. This is motivated by the tuning of the NMPC to be very reactive on smooth roads and friction transition but perhaps too aggressive on rough roads. Jerk performance is also notably affected; however, one could argue that the difference is minor as the ride is already rough. All in all, possible concerns related to model mismatch caused by system variability and noise, were well addressed by simulation on rough roads. As showed by the brake distance and ABS efficiency metrics, deceleration-wise degradation is within the target identified by the benchmark controller. The transient performance gain is also retained as underlined by the peak-to-peak indicators.

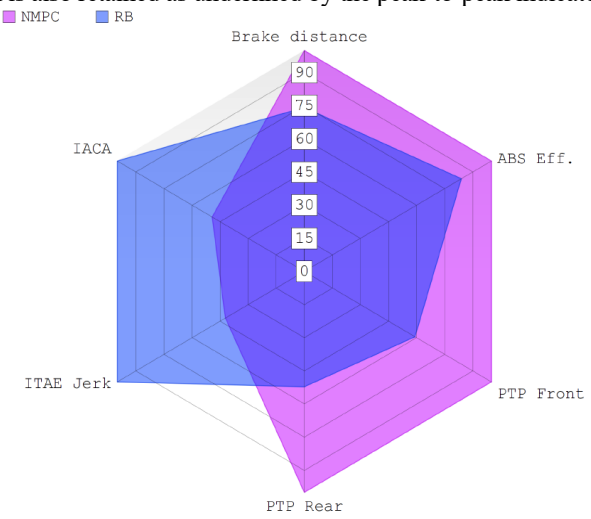

Fig. 7. Rough road braking on belgian stones – Relative KPI readings

VI. Conclusions

The analysis showed that the proposed logic generally outperforms the rule-based control on each of the simulated manoeuvres. The improvements are mainly due to a much smoother and precise control action which destabilizes the wheel dynamics much less than the current logic does with its repeated control cycles (increase, decrease, and hold pressure). Transient behaviour was found to be the main improvement point thanks the optimization of the system's predicted behaviour. On average, based on the three smooth road manoeuvres, the first ABS control cycle was found to be around 75% better than for the rule-based controller. Similarly, following a jump in the friction coefficient, the NMPC was shown to be approximately 50% faster to recover from the friction jump. Steady state tracking was also improved by an average of 15%. Additionally, again thanks to smoother and more precise control action, the velocity at which the controller needed to be switched to low speed mode was reduced by around 50% [13]. Lastly, occupants' comfort was also enhanced and actuator abuse demonstrated to be within what is caused by the benchmark.

Regarding robustness aspects, no issues were found with the optimization problem failing to find a solution. Moreover, the proposed control strategy proved to recover from friction jumps faster than the benchmark and with significantly lower vehicle jerk and yaw rate. Furthermore, the Nonlinear Model Predictive controller showed lower performance degradation levels related to noise injection by the road profile. Minor real-time concerns where highlighted at the beginning of the braking manoeuvre as well as for the first few milliseconds after a friction jump occurred. Causes were identified; however, considering the controller was not run on dedicated hardware, it was decided to leave this point open for future investigations. Lastly, it is worth recalling that the NMPC comes with a considerably lower number of tuning parameters (roughly two order of magnitude lower than the equivalent rule-based logic).

In conclusion, this research proved the application of Nonlinear Model Predictive approach in the field of anti-lock braking control to be extremely promising, and motivates future research targeted at clarifying all those points that remain open. Despite the extent of this work, the conclusions drawn are applicable only to pure longitudinal dynamics context, nonetheless the use of wheel force information and the model-based approach undoubtedly simplifies the extension of the controller to a more general context.

Acknowledgments

The research leading to these results was supported by Toyota Motor Europe (TME) which is hereby greatly acknowledged.

References

[1] S. Savaresi and M. Tanelli, Active Braking Control Systems Design for Vehicles. Springer, second ed., 2012.

[2] M. Schinkel and K. Hunt, "Anti-lock braking control using a sliding mode like approach," in *Proceedings of the 2002 American Control Conference* vol. 3, pp. 2386–2391 vol.3, 2002.

[3] W. Pasillas-Lépine, "Hybrid modeling and limit cycle analysis for a class of five-phase anti-lock brake algorithms," *Vehicle System Dynamics*, vol. 44, no.2, pp. 173–188, 2006.

[4] S. M. Savaresi, M. Tanelli, C. Cantoni, D. Charalambakis, F. Previdi, and S. Bittanti, "Slip-deceleration control in anti-lock braking systems," *IFAC Proceedings Volumes*, vol. 38, no.1, pp. 103–108, 2005. 16th IFAC World Congress.

[5] M. Gerard, W. Pasillas-Lepine, E. de Vries, and M. Verhaegen, "Adaptation of hy- brid five-phase abs algorithms for experimental validation," *IFAC Proceedings Volumes*, vol. 43, no. 7, pp. 13 – 18, 2010. 6th IFAC Symposium on Advances in Automotive Control.

[6] S. Kerst, B. Shyrokau, and E. Holweg, "Reconstruction of wheel forces using an intelligent bearing," *SAE Int. J. Passeng. Cars – Electron. Electr. Syst.*, vol. 9, pp. 196–203, 04 2016.

[7] S. Kerst, B. Shyrokau, and E. Holweg, "A Model-based approach for the estimation of bearing forces and moments using outer ring deformation," *IEEE Transactions on industrial electronic.*, 2019

[8] F. Pretagostini, "A survey on antilock braking systems control strategies," tech. rep., TU Delft, 2018.

[9] V. Ivanov, D. Savitski, and B. Shyrokau, "A survey of traction control and anti-lock braking systems of full electric vehicles with individually-controlled electric motors," *IEEE Transactions on Vehicular Technology*, vol. 64, no. 9, pp. 3878–3896, 2015.

[10] D. Ariens, B. Houska, H. Ferreau, and F. Logist, *ACADO for Matlab User's Manual*. Optimization in Engineering Center (OPTEC), 2010. http://www. acadotoolkit.org/.

[11] H. J. Ferreau, C. Kirches, A. Potschka, H. G. Bock, and M. Diehl, "qpoases: a parametric active-set algorithm for quadratic programming," *Mathematical Programming Computa- tion*, vol. 6, pp. 327–363, 2014.

[12] B. Houska, H. J. Ferreau, and M. Diehl, "An auto-generated real-time iteration algorithm for nonlinear mpc in the microsecond range," *Automatica*, vol. 47, no. 10, pp. 2279–2285, 2011.

[13] F. Pretagostini, "Antilock braking control design using a nonlinear model predictive approach and wheel force information," Master's thesis, TU Delft, https://repository.tudelft.nl/FPretagostini_MScThesis, 2018.

[14] H. Pacejka, *Tire and Vehicle Dynamics*. Butterworth-Heinemann, third ed., 2012.